Electron-energy-loss characterization of laser-deposited *a*-C, *a*-C:H, and diamond films

Peter Kovarik, E. B. D. Bourdon, and R. H. Prince
Department of Physics and Astronomy, York University, Toronto, Ontario, Canada
(Received 29 March 1993)

Electron-energy-loss spectroscopy has been used to identify microcrystalline diamond films produced by laser ablation of graphite. The production of the diamond phase results from varying the deposition geometry and parameters from those of an earlier configuration that produced diamondlike carbon films. A complete study of these crystalline and amorphous materials indicates a plasmon energy variation for films produced in different environments. Spectra taken with different primary energies show variation in the plasmon energy in hydrogenated carbon films. These changes were interpreted as a variation in the bonding nature of the sample with depth. The spectra of all samples were analyzed to determine sp^2/sp^2+sp^3 fraction, dielectric functions, and optical band gap.

I. INTRODUCTION

Laser ablation of graphite has recently been successful in the deposition of diamondlike carbon (DLC) and also diamond films on fused silica substrates.[1,2] These materials have more commonly been deposited from hydrocarbon gases diluted in hydrogen, using various chemical vapor deposition (CVD) methods. The pure laser method allows interesting variations in the growth environment, since the carbon and hydrogen sources can be independently controlled; furthermore, the laser radiation itself can be used at the growth interface to provide surface or gas phase modification.

Amorphous carbon (*a*-C) and hydrogenated amorphous carbon (*a*-C:H) films produced by laser ablation of graphite have been characterized by Fourier-transform infrared spectroscopy (FTIR), scanning electron microscopy (SEM), ultraviolet-visible transmission spectroscopy (UV-VIS), and Raman spectroscopy.[1] These films have been found to be similar to films produced by other, more conventional, CVD methods. Carbon films deposited on fused silica substrates in a hydrogen environment and at elevated surface temperature were found to have a crystalline morphology by SEM and the lattice parameters of diamond, using selected area diffraction. The present paper is a complete study of these laser-deposited materials by electron-energy-loss spectroscopy (EELS). These data are used to discuss the films' electronic structure, microstructure, and resulting optical dielectric function and band gap.

II. EXPERIMENT

The deposition techniques have been given elsewhere[1-3] and are described here briefly. Amorphous carbon was produced by pulsed excimer laser (308 nm) ablation of spectroscopic grade graphite rod in a vacuum environment of less than 1 mTorr. The laser radiation, having pulse energy between 150 and 250 mJ, was focused onto the graphite target at an angle of 30° from the surface normal using a 15-cm focal length lens. Substrates were held approximately 0.64 cm from the target surface in a parallel orientation [Fig. 1(a)]. Hydrogenated amorphous carbon films were prepared by admitting research grade hydrogen gas up to a system pressure of 5 Torr.

Microcrystalline samples were deposited such that the laser beam ablated the graphite target while simultaneously processing the substrate and growing film. This new technique required the fused silica substrate to be placed in the laser beam path before the graphite target, with the two surfaces parallel and 7 cm apart [Fig. 1(b)]. Substrates were abraded with 0.25-μm diamond spray

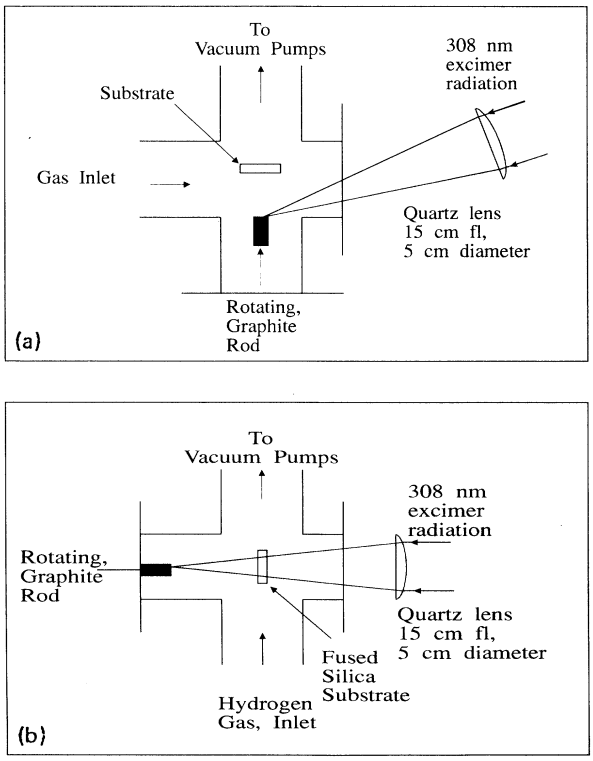

FIG. 1. Schematic representation of deposition setup for *a*-C, *a*-C:H (a), and for microcrystalline diamond (b).

and thoroughly washed in methanol. After clamping substrates in a holder and outgassing at 400 °C and 10^{-5} Torr, the system pressure was raised to 10 Torr of hydrogen flowing at about 6 liters per minute. Deposition temperature was held constant at selected values between 150° and 280 °C; results presented here refer to crystallites typically 2 μm in size, deposited at 280 °C.

Electron-energy-loss experiments were carried out in an ion pumped vacuum chamber maintained at 5×10^{-10} Torr and equipped with a turbo pumped load-lock for rapid sample changes. The backscattered electron energy distribution was measured with a single-pass Varian cylindrical mirror analyzer (CMA) having an integral electron gun and a continuous dynode (Channeltron®) electron multiplier connected for pulsed counting detection. A personal computer system controlled the analyzer pass energy using a digital to analog converter. The multiplier signal was input to a pulse amplifier/discriminator and nuclear counter which was interfaced to the computer. The primary beam energy ranged between 200 and 700 eV, giving an energy resolution between 1 and 2 eV. The electron beam current at the target was kept low at approximately 50 nA, to minimize charging. The typical maximum count rates were 100 000 counts/eV for the elastic peak and 20 000 counts/eV for the plasmon loss features. EELS from standard materials were used to calibrate the spectrometer system and to check the analysis technique.

Samples were held by stainless-steel clips spot-welded to a stainless-steel plate which was transferred to the system's sample manipulator. Highly oriented pyrolytic graphite (HOPG), used as a reference material, was cleaved in air prior to installation into the vacuum chamber. Reference samples of 0.25-μm diamond and 1-μm β-SiC powder were produced by pressing the particles into a high-purity copper foil. This provided an effective way of holding relatively thick (0.2 mm) powder aggregates without any contaminating chemical binders. Sample temperature was monitored via a tungsten–tungsten/rhenium thermocouple attached to the manipulator backplate. In this way, samples could be outgassed or thermally modified at temperatures up to 800 °C.

III. RESULTS AND DISCUSSION

The graphs shown in the following figures all represent unsmoothed data, normalized to the elastic peak, with the elastic peak subsequently removed to improve the scaling of the figures. The typical count rates of the loss features (20 000 counts/eV) represent less than 1% standard deviation statistics.

EELS of HOPG, CVD diamond, and β-SiC

Electron-energy-loss spectra for the reference materials HOPG, CVD diamond, and β-SiC are presented in Fig. 2. Spectra from HOPG showed loss features at 7 and 27 eV, which represent the collective excitations of two groups of valence electrons present in the sp^2 bonded system. The first is a π plasmon due to the π electrons alone and the latter is the $\sigma+\pi$ plasmon due to all valence electrons.[4] The plasmon energies predicted for the HOPG by

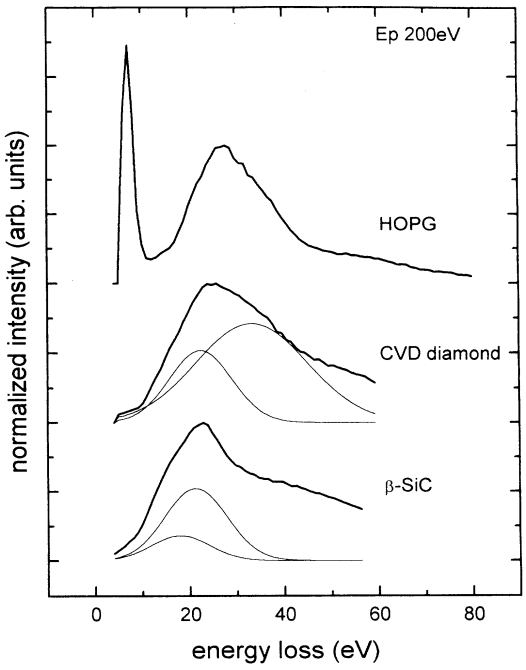

FIG. 2. EELS spectra of the reference materials. CVD diamond and β-SiC are resolved into Gaussian components.

the free electron model,

$$\omega_p = \left[\frac{4\pi n_e e^2}{m}\right]^{1/2}, \tag{1}$$

where n_e is the electron density of the material and m and e are the electronic mass and charge,[5] are pushed apart by the plasmon interaction with the interband transitions of each group of electrons. In addition to the two plasmons, there were much weaker losses at multiple energies due to plural scattering at 14, 21, and 55 eV. The observed energies of the plasma losses are consistent with previously accepted values obtained using the same experimental setup and incident energies.[6]

The loss features occurring at 24 and 33 eV for CVD diamond are assigned to surface and bulk plasmons, respectively. Similar assignments for β-SiC occur at 18 and 23 eV. The surface plasmon energy of the CVD diamond appears very close to $1/\sqrt{2}$ times that of the bulk plasmon, as predicted on the basis of the change in the dielectric constant at the solid/vacuum interface.[5] Both samples show an increase in the magnitude of the bulk plasmon signal as the primary beam energy is increased to 500 eV and the escape depth of electrons increases. EELS from a diamond sample prepared from a 0.25-μm particle spray shows losses consistent with those found for the CVD sample. These plasma loss energies are in agreement with the previously accepted values.[7,8]

EELS of laser deposited carbon films

The loss spectrum of the a-C sample in Fig. 3 displays loss features at 6 and 23 eV, attributed to the π and $\sigma+\pi$ plasma losses of graphite. The main $\sigma+\pi$ plasmon ap-

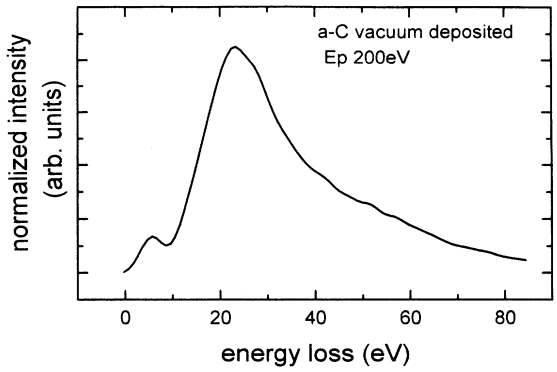

FIG. 3. EELS spectrum of vacuum-deposited a-C film.

pears at the reduced energy as compared to HOPG, reflecting the lower atomic density of the material.

The a-C:H sample shows variations in the loss spectra as the incident electron energy, and hence probing depth, is changed. The mean free path of the electrons is estimated from the universal curve[9] to change from 5 to 15 Å over the primary beam energy range used (200 to 500 eV). Figures 4(a) and 4(b) give typical loss spectra for 200 and 500 eV incident energies, respectively. The $\sigma+\pi$ plasmon is at 31 eV for the 200-eV primary beam, while the same feature appears at 26 eV for the 500- and 700-eV beams. The 5-eV variation in the main plasmon is attributed to a higher sp^3 electron density near the surface, since the 31-eV loss approaches that of diamond. Similarly, the π plasmon shift, from 6 to 5 eV as the incident electron energy is lowered, indicates a decrease in the sp^2 electron density near the surface.

Extended heating of the sample at 700 °C leads to a loss of hydrogen which was monitored by a quadrupole mass spectrometer; the resulting spectra are shown in Fig. 5. The near-surface spectrum, obtained at the 200-eV primary beam energy, shows a reduction in the $\sigma+\pi$ plasmon energy to 26 eV. The $\sigma+\pi$ plasmon at higher incident energies of 500 and 700 eV, shown in Fig. 5(b), shifts downward only slightly to 25 eV. Thus, after the heating, spectra taken at various primary beam energies appear to be similar. The reduction of the plasmon energy indicates a lower electron density and a transformation to a less ordered structure as hydrogen is lost from the sample. These results were corroborated by the reduced intensity of the C-H stretch feature in the FTIR spectra observed during heating of this class of film.

The energy loss spectra of the laser-formed microcrystalline diamond sample, shown in Fig. 6, shows a composite peak containing a number of separate loss features. Gaussian deconvolution isolates a small loss at 18 eV, as well as losses at 23 and 33 eV. The positions and the relative magnitudes of these components suggest that the sample contains β-SiC (18 and 23 eV) and diamond (23 and 33 eV). The unique high-energy position of the 33-eV loss provides a clear identification of diamond present in the film. The interpretation of the components is supported by the increase in the prominence of the 33-eV plasmon loss with an increase in the primary beam energy to 500 eV, similar to that observed for the diamond reference sample.

These results are also consistent with the findings obtained by selected area diffraction (SAD) and scanning electron microscopy given in an earlier report.[1] The

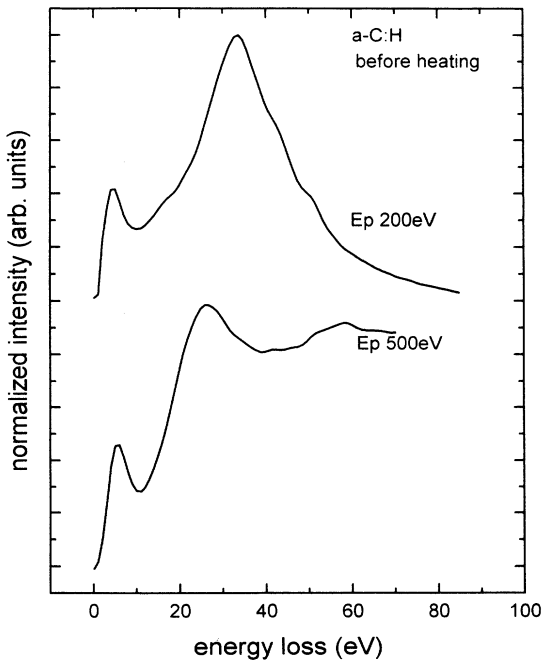

FIG. 4. EELS spectra of a-C:H film taken at $E_p=200$ and 500 eV, before heating.

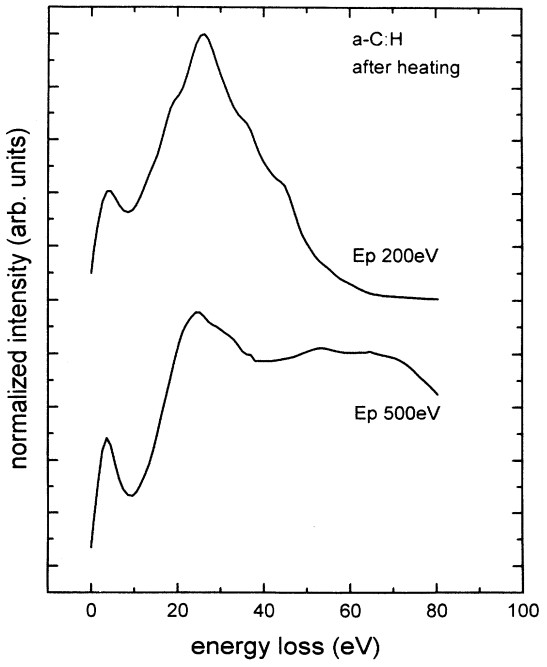

FIG. 5. EELS spectra of a-C:H film taken at $E_p=200$ and 500 eV, after heating.

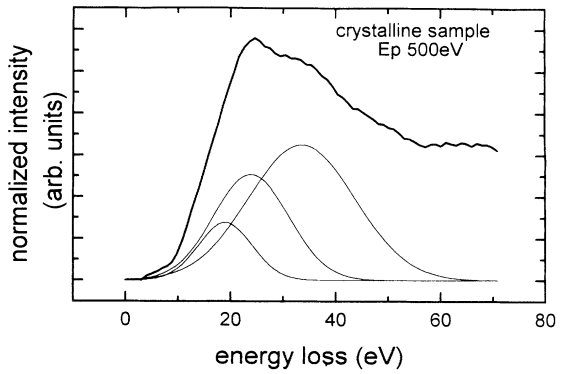

FIG. 6. EELS spectrum of microcrystalline sample resolved into Gaussian components.

SAD of the microcrystalline sample is shown in Fig. 7 (region *C*) along with the diffraction pattern of reference materials, 1-μm β-SiC powder (region *A*) and 0.25-μm diamond spray (region *B*). From the microdensitometer profile of the diffraction pattern, it is estimated that there is 65% diamond and 35% β-Sic in the interface region.[2]

The EELS spectrum of the fused silica substrate surface outside the deposit area shows a 7-eV loss which is assigned to the electronic transition typical of a silicon-rich surface.[10] This further supports the idea that within the deposit area the surface is covered with β-SiC, acting as a precursor to diamond growth

Analysis of EELS

Analysis of the EELS spectra can be extended beyond plasmon loss energies to the determination of the dielectric function. The spectra corrected for the multiple scattering, surface losses, and instrumental broadening

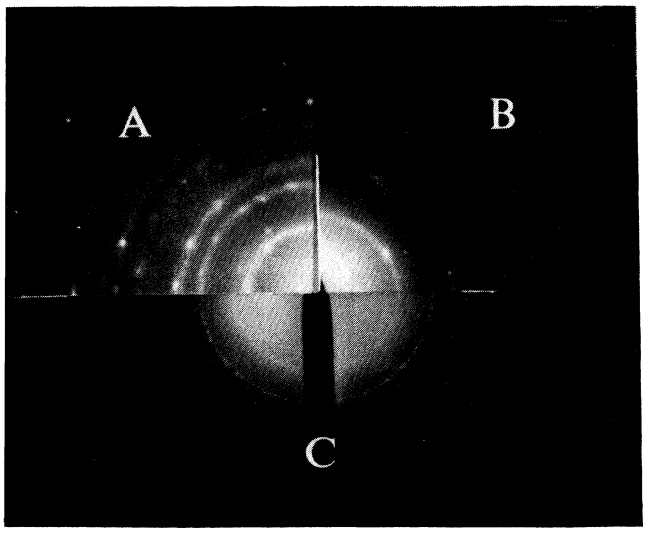

FIG. 7. SAD photograph of microcrystalline sample (c); reference materials are shown: (a) β-SiC powder and (b) diamond spray.

are proportional to $\mathrm{Im}[-1/\epsilon(E)]$.[6] This loss function in turn can be used to generate both parts of the dielectric function using the Kramers-Kronig (KK) relationship relating the imaginary and real parts of the dielectric function,[11]

$$\mathrm{Re}\left[\frac{1}{\epsilon(E)}\right]=1-\frac{2}{\pi}\mathrm{P}\int_0^\infty \mathrm{Im}\left[-\frac{1}{\epsilon(E')}\right]\frac{E'dE'}{(E'^2-E^2)}\ , \tag{2}$$

where P denotes the principal value of the integral.

The KK analysis of the EELS spectra collected with a transmission electron microscope is well established and formed the basis for the present analysis using a CMA instrument. The effects of reflection geometry and lower primary beam energy of the CMA experiments on the KK analysis have been recently discussed by Ohno.[6,12] In this geometry, the incident electron undergoes an elastic collision producing a reflected beam, followed or preceded by an inelastic event leading to the characteristic energy loss. It has been established that the CMA-EELS spectra, collected with primary beam energies of 500 eV and higher, are dominated by inelastic events occurring at small scattering angles, thereby satisfying the dipole approximation and validating a KK analysis.[6] This justifies our present KK analysis of the loss function obtained with a CMA instrument. The dipole approximation at low incident energies (i.e., between 200 and 500 eV) for this collection geometry is still believed to be valid. An estimate based on the expression relating the scattering cross section of the electrons, their angular distribution, and primary electron beam energy[6] shows that at least 70–80 % of inelastic collisions still occur with the momentum transfer of order $\Delta q \sim 0.5$ Å^{-1}. A similar result, showing a small momentum transfer for low primary beam energies, has been obtained for aluminum by Ohno.[6] Even though there is some relaxation of the dipole selection rules in comparison with the higher primary energies, the results of the KK analysis provide a useful estimate for the characterization of the surface. Analysis of two such spectra were performed for the *a*-C:H sample.

The method for evaluating the KK relationship used here followed the approach described by Egerton.[11] The dielectric function, once known, was used to evaluate the sp^2/sp^2+sp^3 ratio, using the Bethe sum rule.[13,14]

The $n(E)$ indicates the number of electrons contributing to the losses up to the energy E,

$$n(E)=\frac{m}{2\pi^2e^2N}\int_0^E E'\epsilon_2(E')dE'\ , \tag{3}$$

where N is the density of the atoms of the material and $\epsilon_2(E)$ is the imaginary part of the dielectric function. The method of analysis is first verified for the reference materials HOPG and CVD diamond, and is then applied to the laser prepared films; the derived results are compared to those of other independent methods.

The KK analysis of HOPG yields the dielectric function shown in Fig. 8(a). The 4-eV peak in ϵ_2 corresponds to the π transitions, while the 12-eV peak represents the

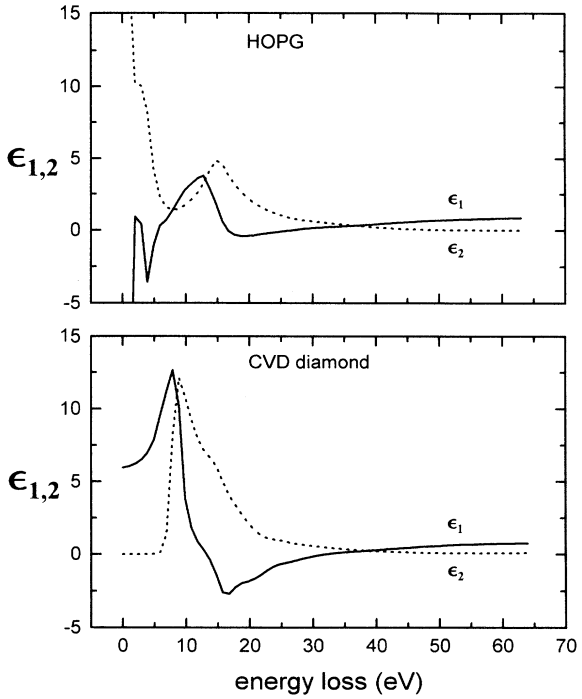

FIG. 8. Components of the dielectric function obtained for HOPG and CVD diamond.

σ transitions. The peak positions agree to within 1 eV and the magnitudes within 20% with the optical results of Taft and Phillipp.[4] The π transition oscillator causes the zero crossing in the real part of the dielectric function, thus leading to the first peak of the loss function.[15] The well-defined separation between the π losses and $\sigma+\pi$ losses at 8 eV allows the evaluation of the number of π electrons, hence the sp^2/sp^2+sp^3 ratio.[13,14] For HOPG this ratio is found to be $\frac{1}{4}$, verifying the KK analysis method and use of the sum rule. The material band gap is estimated using extrapolation of the relationship[15]

$$E^2\epsilon_2(E)=k(E-E_{bg})^2 , \tag{4}$$

where E_{bg} represents the band gap and k is a material specific constant. For HOPG the method indicates a 0.0 ± 0.1-eV energy gap.

Analysis of the CVD diamond sample provided a verification for the method used to extract the band gap from the dielectric function. The KK analysis is applied to the 500-eV primary energy spectrum; the results are given in Fig. 8(b). The dielectric function shows a zero crossing characteristic of an insulating material. The imaginary part of the dielectric function is zero over the range of π transitions, thus confirming the expected sum rule result of no sp^2 content in the sample. The band gap of 5.5 ± 0.5 eV was obtained from $\epsilon_2(E)$ for the CVD diamond sample, and 1.7 ± 0.1 eV for the β-SiC sample.

KK analysis for the a-C sample shown in Fig. 9 indicates a small sp^3 content of $(20\pm10)\%$, thought to be due to the amorphous regions surrounding the sp^2 bonded regions. Based on $\epsilon_2(E)$, a band gap of 0.0 ± 0.1 eV is

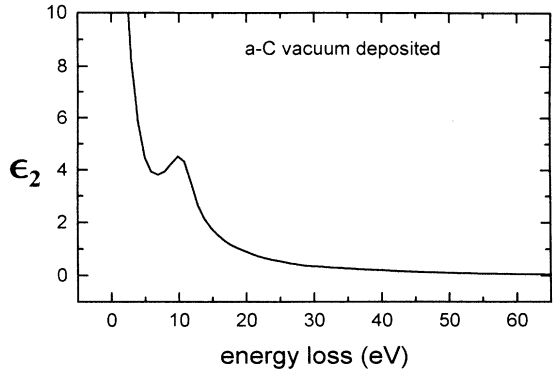

FIG. 9. Imaginary part of the dielectric function obtained for a-C film.

determined for the a-C sample; within error limits, this value is close to the 0.14-eV gap found by VIS-UV measurements reported previously.[11] The amorphous tetrahedral matrix between graphitic clusters arises from condensation of the highly nonequilibrium plasma induced by the high-energy input from the UV laser radiation. The impingement of high energy ions is a means of selectively sputtering graphitic regions, while thermal energy produced at the growth interface will also influence the size of graphitic clusters that form.

The a-C:H sample shows a significant shift in the bulk plasmon energy as the primary energy is varied, indicating a change in the nature of the material with sampling depth. KK analysis has been carried out for loss functions at low and high incident electron energies as shown in Fig. 10(a).

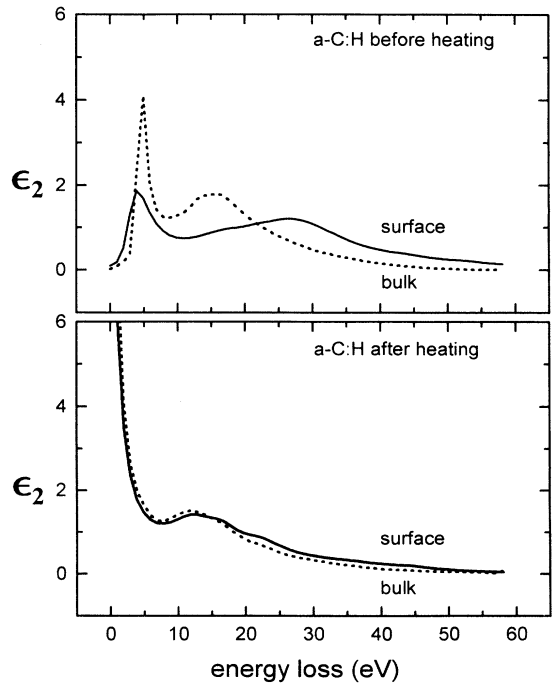

FIG. 10. Imaginary part of the dielectric function obtained for a-C:H film surface and bulk, before and after heating.

The sp^2/sp^2+sp^3 ratio for the a-C:H films from the KK analysis is corrected for the 37% atomic hydrogen content in these films determined by elastic recoil spectroscopy.[16] Evaluation of the dielectric function for both loss functions allows a comparison between the surface and bulk sp^2 fractions. As the primary beam energy is decreased, the sp^2 content is found to decrease from 40% to 25%. The band-gap estimates from $\epsilon_2(E)$ are 1.6±0.1 eV near the surface and 1.2±0.1 eV within the bulk. These values correlate with the 1.56-eV value found by an optical transmission measurement.[1]

After extended heating of the a-C:H film at 700 °C and the associated expulsion of hydrogen, $\epsilon_2(E)$ shown in Fig. 10(b) becomes similar to that of a-C, indicating a reduction of the sp^3 content as well as a closing of the band gap. The sp^2 fraction of the bulk increases to 65%, while the surface fraction approaches 55% sp^2; the band gap in both cases becomes 0.0±0.1 eV. The observed hydrogen loss is concomitant with the reversion of this a-C:H film to a vacuum-deposited-type material shown earlier in Fig. 5. The hydrogen plays a stabilizing role in the formation of the sp^3 bond, and higher hydrogen content near the surface explains the difference between the sp^2 fraction of the surface and bulk of the film before heating. The hydrogen atoms saturate the carbon bonds at the growth surface leading to larger degree of tetrahedral bonding. Surface H atoms would be replaced by C atoms or C-H radicals as the film grows, increasing the C content as the surface gets incorporated into the bulk. During heating, the H atoms from the bulk diffuse through the surface layer, leading to the higher H content and sp^3 fraction seen at the surface during the experiment. This is in agreement with the role of hydrogen in films produced by more conventional techniques, which indicate an increase in sp^3 content with increasing H concentration.[17]

To isolate the loss function for the microcrystalline diamond sample, the higher primary beam energy data showing a prominent bulk loss feature are used, after removal of the surface loss and β-SiC features. The β-SiC part of the spectrum is taken from the reference loss function obtained for that material at 500-eV primary beam energy. The resulting loss function isolates the loss at 33 eV as shown in Fig. 11, and indicates dielectric curves similar to those obtained for CVD diamond shown in Fig. 8(b).

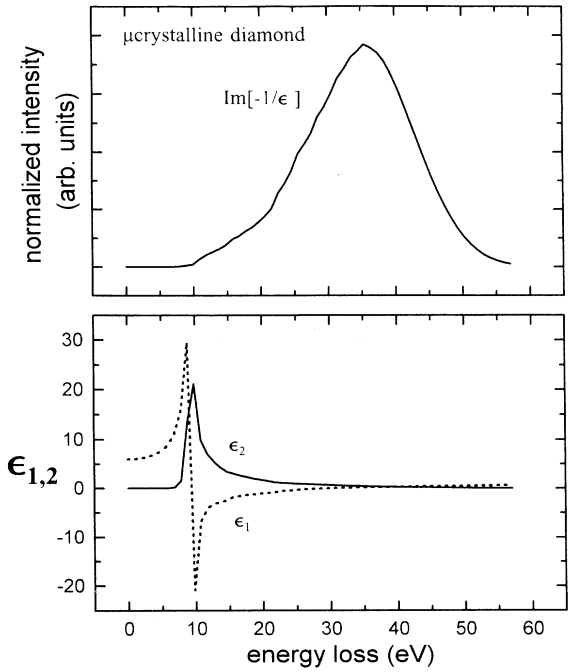

FIG. 11. The isolated loss function of the microcrystalline diamond sample and the resulting dielectric function.

A full summary of all the EELS data and analysis is given in Table I.

TABLE I. Summary of EELS results and analysis. a-C:H(1) sample before heating; a-C:H(2) sample after heating. (s) denotes surface; (b) denotes bulk.

	ΔE plasmon		ΔE plasmon	sp^1,sp^2 (%)	Band gap (eV)
HOPG	7 eV	π	27 eV $\sigma+\pi$	(100±10) sp^2	0.0±0.1
CVD diamond	24 eV	surface	33 eV bulk	(100±10) sp^3	5.5±0.5
β-SiC	18 eV		23 eV bulk		1.7±0.1
a-C	6 eV	π	23 eV $\sigma+\pi$	(80±10) sp^2	0.0±0.1
a-C:H(1) Ep 200 eV	5 eV	π	31 eV $\sigma+\pi$	(25±5) sp^2	1.6±0.1
a-C:H(1) EP 500 eV	6 eV	π	26 eV $\sigma+\pi$	(40±5) sp^2	1.2±0.1
a-C:H(2) Ep 200 eV	6 eV	π	26 eV $\sigma+\pi$	(55±5) sp^2	0.0±0.1
a-C:H(2) EP 500 eV	6 eV	π	25 eV $\sigma+\pi$	(65±7) sp^2	0.0±0.1
micro-crystalline sample	18 eV 23 eV	β-SiC β-SiC	23 eV diamond (s) 33 eV diamond (b)	(100±10) sp^3 (diamond)	5.0±0.5

IV. CONCLUSION

EELS provides an excellent diagnostic tool for the characterization of DLC and diamond films. Implementation in an Auger CMA system makes the technique readily available to most surface science laboratories. The data presented have shown the laser-deposited amorphous films to have the structure of a carbon material with varying degrees of tetrahedral bonding occurring between graphitic regions; even without the presence of hydrogen in the growth environment, laser ablation of graphite produces films with 15–20 % tetrahedral bonding, resulting in a small optical band gap. During condensation from the highly excited laser-induced carbon plasma, ion bombardment and thermal energy at the growth interface act to control clustering and the size of graphitic regions. Hydrogen is easily incorporated in the films and results in an increased tetrahedral bonding character and increased optical band gaps of up to 1.5 eV. An interesting result has been identified through the enhanced surface sensitivity of the EELS geometry used at lower primary energies, namely, that tetrahedral coordination of carbon atoms is found to predominate at the surface of *a*-C:H films, presumed to be stabilized by hydrogen atoms. This strongly supports the role of hydrogen atoms in the growth surface of diamond films. EELS of the crystalline films produced by the laser method has provided additional evidence for the occurrence of the diamond phase in these carbon films. Work in progress will concentrate on the line-shape analysis of Auger spectra in order to determine the density of states for these materials.

[1]E. B. D. Bourdon, W. W. Duley, A. P. Jones, and R. H. Prince, Surf. Coat. Technol. **47**, 509 (1991).
[2]E. B. D. Bourdon, P. Kovarik, and R. H. Prince, Diamond Relat. Mater. **2**, 425 (1993).
[3]E. B. D. Bourdon and R. H. Prince, U.S. Patent Appl. Ser. No. 821,416 (filed 14 January 1992); Canadian Patent Appl. Ser. No. 2059185-4 (filed 10 January 1992).
[4]E. A. Taft and H. R. Phillipp, Phys. Rev. **138**, A197 (1965).
[5]F. Wooten, *Optical Properties of Solids* (Academic, New York, 1972), pp. 63 and 221.
[6]Y. Ohno, Phys. Rev. B **39**, 8209 (1988).
[7]P. G. Luri and J. M. Wilson, Surf. Sci. **65**, 476 (1977).
[8]R. Kaplan, Surf. Sci. **215**, 118 (1989).
[9]A. Zangwill, *Physics at Surfaces* (Cambridge University Press, Cambridge, England, 1988), p. 21.
[10]U. Buechner, J. Phys. C **8**, 2781 (1975).
[11]R. F. Egerton, *Electron Energy-Loss Spectroscopy in the Electron Microscope* (Plenum, New York, 1986).
[12]Y. Ohno, Phys. Rev. B **36**, 7500 (1987).
[13]J. Fink, Th. Muller-Heinzerling, J. Pfluger, B. Scheere, B. Dischler, P. Koidl, A. Bubenzer, and R. E. Sah, Phys. Rev. B **30**, 4713 (1984).
[14]J. Fink, Th. Muller-Heinzerling, J. Pfluger, A. Bubenzer, P. Koidl, and G. Cucellins, Solid State Commun. **47**, 687 (1983).
[15]J. Fink, *Advances in Electronics and Electron Physics,* edited by P. W. Hawkes (Academic, New York, 1989), Vol. 75, p. 122.
[16]E. B. D. Bourdon, A. Raveh, and L. Martinu (unpublished).
[17]J. C. Angus, Thin Solid Films **216**, 126 (1992).

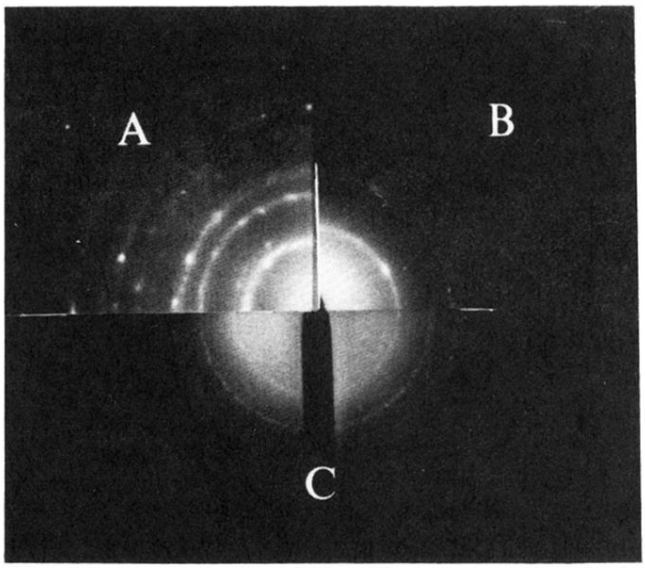

FIG. 7. SAD photograph of microcrystalline sample (c); reference materials are shown: (a) β-SiC powder and (b) diamond spray.